

Spinning Reserve Requirement Optimization Considering Integration of Plug-in Electric Vehicles

Jian Zhao, *Student Member*, Can Wan, *Member, IEEE*, Zhao Xu, *Senior Member, IEEE*, Kit Po Wong, *Fellow, IEEE*

Abstract—The increasingly widespread utilization enables plug-in electric vehicles (PEVs) to provide ancillary service and support economic and secure operation of power systems. This paper proposes a novel model to optimize day-ahead spinning reserve requirement (SRR) considering PEVs' contribution in providing operating reserve. Based on the probabilistic criteria, the cost of expected energy supplied by PEV (EESEV) is formulated. The costs of reserves from traditional generators and PEVs as well as expected energy not supplied (EENS) are considered together to determine optimal spinning reserve requirement. The post-contingency PEV reaction time is taken into account in the formation of EENS and EESEV. The capacities of PEV interruptible charging demand and vehicle to grid (V2G) service are calculated respectively under the conditions of both immediate charging and smart charging strategies. The effects of PEVs on system spinning reserve requirement quantification, unit commitment are comprehensively analyzed using IEEE reliability test system (RTS-96). Numerical results systematically demonstrate the effectiveness of PEVs' participation on the reduction of operation costs and the improvement of power system reliability. Sensitivity analysis of PEV penetration level and compensation cost to PEV owners is compressively conducted to provide meaningful reference for future implementation.

Index Terms—Spinning reserve requirement, expected energy not supplied, plug-in electric vehicle, expected energy supplied by electric vehicle, vehicle to grid

NOMENCLATURE

Sets:

G	Set of generators.
T	Set of hourly time intervals.
T_d	Set of intra-hour time intervals.
V	Set of PEVs.
V_c	Set of PEV clusters.

Parameters

C_{BI}	Battery investment cost of V2G service [\$/kWh].
C_{Comp}	Compensation cost paid to PEV owners [\$/MWh].
C_{Int}	Cost of interrupted PEV charging demand

This work was partially supported by Hong Kong Research Grants Council Theme Based Research Scheme Grant no. T23-407/13N and T23-701/14N, National High-tech R&D Program of China (863 Program, grant no. 2014AA051901), China Postdoctoral Science Foundation grant no. 2015M580097, and National Natural Science Foundation of China grant no. 51207077, and 51261130472.

J. Zhao, C. Wan and Z. Xu are with Dept. of Electrical Engineering, The Hong Kong Polytechnic University, Hung Hom, Hong Kong. C. Wan is also with Dept. of Electrical Engineering, Tsinghua University, Beijing 100084, China (e-mail: zhaojianzju@gmail.com, can.wan.hk@iee.org, eezhaoxu@polyu.edu.hk).

K. P. Wong is with School of Electrical, Electronics, and Computer Engineering, University of Western Australia, WA, Australia (e-mail:kitpo@ieee.org).

C_{V2G}	Cost of PEV V2G service [\$/MWh].
CR_{PEV}	PEV compensation rate.
d_{DoD}	Certain depth of discharge.
E_v^{Cons}	Daily energy consumption of PEV v [kWh].
Lb, Ub	Lower and upper bounds of SRR in grid search-based SRR optimization methodology [MW].
L_C	Battery cycle life at a certain depth of discharge.
N_{PEV}	Total number of PEVs.
n_c	Number of PEVs in cluster c .
$ORR_{i,\tau}$	Outage replacement rate of unit i with time τ .
P_{aver}	Average power system demand [MW].
P_t^{CH}	Total PEV charging demand at time t [MW].
P_t^D	Power system demand without PEV charging demand at time t [MW].
$P_{ch,max}$	Maximum charging power of each PEV [kW].
$P_{V2G,max}$	Maximum V2G discharging limitation [kW].
P_i^{min}, P_i^{max}	Lower/Upper limit of power output of unit i [MW].
PL_{PEV}	Penetration level of PEVs in power system.
R_i^{up}	Short-term up-regulation reserve rate of unit i [MW].
RD_i, RU_i	Hourly ramp-up/ramp-down ability of unit i [MW].
$S_{EV,max}$	Capacity of PEVs' battery [kWh].
$S_{clus,min}$	Lower and upper limitations of equivalent SOC (state of charge) of PEV cluster c [kWh].
$S_{clus,max}$	Expected SOC when PEV cluster c plugs out [kWh].
$S_c^{clus,exp}$	Expected SOC when PEV cluster c plugs out [kWh].
t_v^{arr}, t_v^{dep}	Arriving and departing time of PEV v .
$u_{v,t,\tau}^{EV}$	Binary parameter with 1 indicating PEV connected to the grid.
$u_{i,t,\tau}^{CI}, u_{i,t,\tau}^{CH}$ and $u_{i,t,\tau}^{CII}$	Binary parameters with 1 indicating the state before, during and after contingency
$u_{i,t,\tau}^{EV,del}$	Binary parameter with 1 denoting PEV reacting to contingency
$VOLL$	Value of lost load [\$/MWh].
α, β, γ	Coefficients of generator cost function [\$/MW ² \$/MW \$].
$\Delta t, \Delta \tau$	Period of each time interval, $\Delta t = 1$ hour; $\Delta \tau = 10$ minutes.
η_{ch}	PEV charging efficiency.
λ_i	Expected failure rate of unit i .
ξ_t	Uncertainty parameter of PEV behaviors.
τ_1	Post-contingency PEV reaction time interval [h].
τ_2	Power system contingency time interval [h].

ω	Certain proportion of power system demand that is required to provide, used as load following reserve
Variables	
$EENS_t$	Expected energy not supplied [MWh].
$EESEV_t^{int}$	Expected energy supplied by PEVs' charging interruption [MWh].
$EESEV_t^{V2G}$	Expected energy supplied by PEVs' V2G service [MWh].
$ES_{j,t}, ES_{jk,t}$	Energy shift with random event of single unit j outage and double units j and k outage [MWh].
$E_{v,t}^{Ch}$	Total PEV charging energy between when PEV responds to contingency and when system recovers [kWh].
$E_{v,t}^{Sup}$	Maximum supplementary recharging energy between the recovery of power system and the departure of PEVs [kWh].
$E_{v,t}^{Rem}$	Total energy remained in the PEV battery when PEVs conduct V2G service [kWh].
$E_{v,t}^{V2G,lim}$	Energy of V2G limitation during contingency period [kWh].
$P_{i,t}$	Power output of unit i at time t [MW].
P_t^{int}	The power capacity of interruptible PEV charging [MW].
P_t^{V2G}	The power capacity of PEV V2G service [MW].
P_t^{EVR}	Total power capacity of operating reserve that PEVs provide [MW].
$P_{v,t,\tau}^{ch}$	Charging power of PEV v at time t, τ [kW].
P_t^{total}	Total power system demand with PEVs charging demand taken into consideration [MW].
P_{aver}	Average power system demand [MW].
$P_{c,t,\tau}^{ch,clus}$	Equivalent charging power of PEV cluster c at time t, τ [kW].
$Pr_{j,t,\tau}$	Probability of the random event of single unit j outage and double units j and k outage.
$Pr_{jk,t,\tau}$	Probability of the random event of double units j and k outage.
r_t^{req}	Spinning reserve requirement at time t [MW].
$r_{i,t}$	Spinning reserve provided by unit i at time t [MW].
$S_{c,t}^{clus}$	Equivalent SOC of PEV cluster c at time t [kWh].
$u_{i,t}^G$	On/off status of unit i at time t .

I. INTRODUCTION

SPINNING reserve in power systems is defined as the reserve capacity which is spinning, synchronized and prepared to dynamically balance system load [1]. In order to withstand sudden outages of some generators and unforeseen fluctuations of the load and renewable energies [2], the daily operation cost increases because additional generators are committed on and other cheaper generators are operating less than the optimal output to provide the spinning reserve. Due to the widely application of PEVs, PEVs' potential ability of interrupting charging demand and providing V2G service during the power system contingency may benefit the secure and economic operation of power systems. However, the effects of PEVs on the quantification of spinning reserve requirement remain to be further studied.

To quantify the spinning reserve requirement, both

deterministic and probabilistic criteria have been developed to maintain the power system operating within a certain risk level. The reserve set by deterministic criteria is mainly based on the capacity of the largest online generator or the certain proportion of the daily peak load, which is relatively easy to implement [3]. However, various system uncertainties and the stochastic nature of the component failures are not taken into consideration in the deterministic criteria. To overcome this limitation, the probabilistic criteria have drawn lots of attentions due to its advantages on reflecting the uncertainties of the availability of generators, the outages of transmission networks, generator response rate, and so on [4]. The loss of load probability (LOLP), the expected energy not supplied (EENS) and the unit commitment risk (UCR) are widely used as probabilistic criteria to evaluate the system SRR [1]. A market clearing process with bounded LOLP and EENS is proposed as additional linearized constraints of unit commitment (UC) formulation [5]. Market clearing models are proposed in [6] to optimize the spinning reserve via adding the cost of energy deficit calculated by the value of lost load (VOLL) and EENS into the classical UC problem. However, these spinning reserve optimization methods are based on the adjustment of UC formulation, which requires complicated iterative processes or approximate calculation of the risk levels associated with the reserve provision. To address this problem, a cost and benefit analysis model is proposed to optimize the SRR in an auxiliary optimization method before solving the UC problem [7]. The advantage of this model lays not only on the computation burden reduction by avoiding suboptimal solutions but also on the outstanding compatibility with existing UC problems.

In modern power systems, the effects of various factors are considered in the quantification of the SRR. The uncertainty of high penetration of wind power [8] brings a great challenge to optimize the spinning reserve [9, 10]. In addition, other emerging impact factors including carbon capture plants [11], customers' choice on the reliability [12] and bidding uncertainties in the electricity market [13] are taken into account in determining the spinning reserve. To maintain the power system adequacy, some other factors are included to partly replace the spinning reserve such as rapid start units, assistance from interconnected system, interruptible loads, voltage and frequency reductions, and so forth [14]. These additional factors and spinning reserve are regarded as operating reserve. In practice, hydro generation acts as the most common fast start-up unit to provide operating reserve [15]. An energy based technique to assess spinning reserve requirements considering the aid of interconnected systems is presented in [16]. The effects of interruptible load and demand response on spinning reserve quantification are analyzed in [17].

Due to the unique advantages of flexible charging load and V2G service, PEVs can be an effective alternative resource to provide operating reserve in the power system under proper compensation mechanism. With the large-scale application of PEVs in the foreseeable future, the ability of PEVs in providing ancillary service has been attracting tremendous attentions [18-22]. Among these studies, the optimal EV scheduling

schemes or the optimal bidding strategies involved in energy and reserve market are obtained via maximizing the profit of EV aggregators. Especially, power system reserve provided by V2G service can mitigate the effects of wind power production uncertainty and facilitate the integration of wind power [23, 24]. EVs can also provide supplemental primary reserve and frequency regulations through V2G technology to enhance power system stability [25, 26].

A cost-efficiency based optimization model of day-ahead spinning reserve requirement optimization considering the integration of PEVs is proposed in this paper. In the study, PEVs participate in contingency reserve allocation and provide energy support through charging interruption and V2G service when energy deficit happens due to generator outage. Similar to EENS, expected energy supplied by PEV is formulated to quantify PEVs' provision of operating reserve. Comprehensive cost/benefit analysis is executed to compare the reserve provision cost of traditional generators and PEVs. It explicitly verifies the merits of PEVs' reserve provision including the reduction of operation cost and the improvement of system reliability during power system contingency. The impacts of the PEV penetration level and the compensation to PEV owners on SRR allocation are systematically investigated in this paper on basis of sensitivity analysis to provide very useful information to future implementation and effectively bring the concept of V2G into practice. Generally, the main contributions of this paper include the following aspects:

1) Distinguished from existing literatures, PEVs are innovatively considered in the determination of power system SRR in this paper. The costs of reserves from traditional generators and PEVs as well as EENS are taken into account together to determine optimal SRR.

2) The concept of EESEV is innovatively proposed in the study to quantify the expected energy supplied by PEVs. The reaction time of PEVs' reserve provision is taken into account in the calculation of EESEV, as well as EENS.

3) PEVs' capacity of interruptible charging demand and V2G service under both smart charging and immediate charging strategy is formulated in this paper.

4) The effectiveness of PEVs on power system SRR optimization, unit commitment and system reliability is comprehensively investigated under various scenarios.

5) The sensitivity analysis of the PEV penetration level and the compensation to PEVs owners is newly executed to provide meaningful reference for future implementation of PEVs' participation in operation reserve.

The structure of the remainder of this paper is organized as follows. Section II describes the formulation and optimization of SRR considering PEVs' participation, where EENS and EESEV are formulated based on a probabilistic criterion. The modeling of PEVs' providing operation reserve is proposed in Section III, where the capacity and cost of interruptible charging demand and V2G service in different charging strategies are formulated. Case studies for the verification of the proposed model are fulfilled, analyzed and discussed in Section IV. Further discussions on the uncertainties of the future implementation of the proposed model are conducted in Section V. Finally, the conclusion is given in Section VI.

II. FORMULATION AND OPTIMIZATION OF SPINNING RESERVE REQUIREMENT

A. Formulation of Spinning Reserve Requirement

As the model developed in [7], the SRR of each optimization period can be determined using an auxiliary optimization method before solving the UC problem. Hourly SRR is separately optimized for each time interval based on cost/benefit analysis. The inter-temporal constraints are neglected in the optimization model for practical application [7, 9, 11]. Once the hourly SRR is determined, it is used as inputs of traditional reserve-constrained UC model. The main advantage of the model mainly lies in the cost/benefit analysis of reserve provision. It would be beneficial and practical to evaluate the effects of PEVs on spinning reserve requirement from the economic-efficiency perspective. Taking PEVs into consideration, the SRR model is proposed to not only balance the cost of operating generation and the cost of EENS, but also incorporate the cost of the energy supplied by PEVs.

The SRR model with the assistance of PEVs can be formulated as,

$$\min_{r_t^{\text{req}}} f_{\text{SRR}}(r_t^{\text{req}}) = f_{\text{OPER}}(r_t^{\text{req}}) + f_{\text{EENS}}(r_t^{\text{req}}) + f_{\text{EESEV}}(r_t^{\text{req}}) \quad (1)$$

where,

$$f_{\text{OPER}}(r_t^{\text{req}}) = \min_{u_{i,t}^G, P_{i,t}} \sum_{i \in G} \alpha P_{i,t}^2 + \beta P_{i,t} + \gamma u_{i,t}^G \quad (2)$$

$$f_{\text{EENS}}(r_t^{\text{req}}) = \text{VOLL} \times \text{EENS}_t \quad (3)$$

$$f_{\text{EESEV}}(r_t^{\text{req}}) = C_{\text{Int}} \text{EESEV}_t^{\text{Int}} + C_{\text{V2G}} \text{EESEV}_t^{\text{V2G}} \quad (4)$$

subject to:

$$\sum_{i \in G} P_{i,t} - (P_t^{\text{D}} + P_t^{\text{CH}}) = 0, \forall t \in T \quad (5)$$

$$r_t^{\text{req}} - \sum_{i \in G} r_{i,t} \leq 0, \forall t \in T \quad (6)$$

$$r_{i,t} = \min\{u_{i,t}^G (P_i^{\text{max}} - P_{i,t}), u_{i,t}^G R_i^{\text{up}}\}, \forall t \in T, \forall i \in G \quad (7)$$

$$P_{i,t} \geq u_{i,t}^G P_i^{\text{min}}, \forall t \in T, \forall i \in G \quad (8)$$

$$P_{i,t} + r_{i,t} \leq u_{i,t}^G P_i^{\text{max}}, \forall t \in T, \forall i \in G \quad (9)$$

$$-u_{i,t-1}^G \text{RD}_i \leq P_{i,t} - P_{i,t-1} \leq u_{i,t-1}^G \text{RU}_i, \forall t \in T, \forall i \in G \quad (10)$$

The objective function (1) is to minimize the overall hourly cost with respect to the SRR r_t^{req} , consisting of the cost of operating generation $f_{\text{OPER}}(r_t^{\text{req}})$, the cost of the expected energy not supplied $f_{\text{EENS}}(r_t^{\text{req}})$ and the cost of the expected energy supplied by PEV $f_{\text{EESEV}}(r_t^{\text{req}})$. The generation operation cost expressed in (2) is the running cost of generators to serve the demand and provide the amount of SRR r_t^{req} . The cost of EENS defined in (3) is the expected cost compensated to the users due to the load shedding. The cost of EESEV represented in (4) is composed of the cost of interrupting the PEV charging demand and the cost of implementing V2G. The cost for PEVs' interruption and V2G service consists of compensation to PEV owners for delayed charging and the battery degradation, of which the details will be discussed in Section III.

The constraint of electric power balance at each period is expressed as (5). The limitations of the spinning reserve provided by each unit are defined by (6) and (7). The limitations of power generation are shown as (8) and (9), and

the maximum limitation of ramp-up and ramp-down rates of each unit is shown as (10).

B. Formulation of EENS and EESEV

EENS can be obtained based on the installed capacity of generating units, the probability of forced outage of each generating unit, the amount of spinning reserve that each unit can provide and the load level [1]. It is calculated by summing all the curtailed energy associated with the probability of each contingency. When the PEVs take part in the operating reserve, EENS, as well as EESEV should be reformulated to consider the reduction of the shedding load due to the assistance of PEVs. The formulation of EENS and EESEV is complicated as PEVs need some time to take actions. The power not supplied during contingency period is depicted in Fig. 1, where EENS and EESEV are shown by the areas in different colors. PEV reaction time τ_1 is defined as the delayed time for PEV aggregator to take action. To conduct post-contingency dispatch of PEVs, the aggregator should firstly receive PEV reserve dispatching commands from power system operator; at the same time obtain the information of each PEV, e.g. SOC and departure time; finally make decision on each PEV's interruption and V2G energy based on each PEV's urgency priority towards energy. System contingency time τ_2 is defined as the time interval before the contingency reserve is restored by the offline generators. The values of τ_1 and τ_2 are set according to the interruptible import requirement and contingency reserve restoration requirement in Reliability Standards for the Bulk Electric Systems of North America [27]. Then $EENS_t$ can be divided into $EENS_t^I$ and $EENS_t^{II}$, where $EENS_t^I$ is the expected energy not supplied during τ_1 and $EENS_t^{II}$ denotes the expected energy not supplied between τ_1 and τ_2 . Only $EENS_t^{II}$ is reduced due to the existence of the expected energy supplied by the interrupted energy of PEV $EESEV_t^{Int}$ and the expected energy supplied by V2G energy $EESEV_t^{V2G}$.

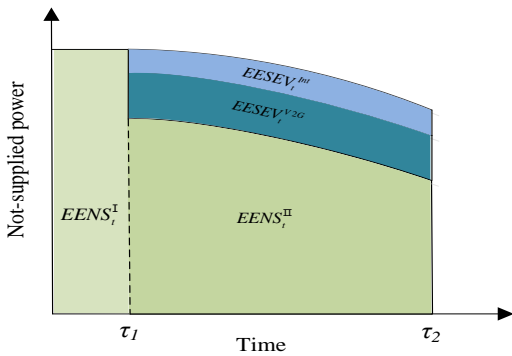


Fig. 1. Area for evaluating EENS, $EESEV_t^{Int}$ and $EESEV_t^{V2G}$

To calculate EENS and EESEV, the probability of capacity outage should be firstly analyzed. The failed probability of a certain generator could be estimated as [1],

$$ORR_{i,\tau} = 1 - e^{-\lambda_i \tau} \approx \lambda_i \tau, \forall i \in G, \tau = \tau_1, \tau_2 \quad (11)$$

where $ORR_{i,\tau}$ is defined as the outage replacement rate and represents the probability that the unit i fails and is not replaced during time interval τ . Then the time-dependent probability of

the random outage event can be obtained by (12) and (13),

$$Pr_{j,t,\tau} = u_{j,t}^G ORR_{j,\tau} \prod_{i \in G, i \neq j} (1 - u_{i,t}^G ORR_{i,\tau}), \forall j \in G, \forall t \in T, \tau = \tau_1, \tau_2 \quad (12)$$

$$Pr_{jk,t,\tau} = u_{j,t}^G ORR_{j,\tau} u_{k,t}^G ORR_{k,\tau} \prod_{i \in G, i \neq j,k} (1 - u_{i,t}^G ORR_{i,\tau}), \tau = \tau_1, \tau_2, \forall j, k \in G, \forall t \in T \quad (13)$$

where $Pr_{j,t,\tau}$ denotes the probability of the random event of single unit j outage, and $Pr_{jk,t,\tau}$ denotes the random event of units j and k outage. It needs to emphasize that the outage events of more than two units are not taken in consideration in the study. The energy shift with these contingency scenarios can be defined as,

$$ES_{j,t} = P_{j,t} - (r_t^{req} - r_{j,t} - \omega P_t^D), \forall j \in G, t \in T \quad (14)$$

$$ES_{jk,t} = P_{j,t} + P_{k,t} - (r_t^{req} - r_{j,t} - r_{k,t} - \omega P_t^D), \forall j \in G, t \in T \quad (15)$$

where ωP_t^D represents the certain proportion of demand that are required to provide, used as load following reserves [28].

For the simplification of the expression of EENS and EESEV, a piecewise function $g(x)$ is introduced and defined as below:

$$g(x) = \begin{cases} x, & \text{if } x \geq 0 \\ 0, & \text{if } x < 0 \end{cases} \quad (16)$$

EENS with the involvement of PEV could be formulated as,

$$EENS_t = EENS_t^I + EENS_t^{II} \quad (17)$$

where

$$EENS_t^I = \sum_{j \in G} Pr_{j,t,\tau_1} g(ES_{j,t}) \tau_1 + \sum_{j \in G} \sum_{k \in G, j < k} Pr_{jk,t,\tau_1} g(ES_{jk,t}) \tau_1, \forall t \in T \quad (18)$$

$$\begin{aligned} EENS_t^{II} = & \sum_{j \in G} Pr_{j,t,\tau_2} g(ES_{j,t} - P_t^{EVR}) \tau_2 \\ & + \sum_{j \in G} \sum_{k \in G, j < k} Pr_{jk,t,\tau_2} g(ES_{jk,t} - P_t^{EVR}) \tau_2 \\ & - \sum_{j \in G} Pr_{j,t,\tau_1} g(ES_{j,t} - P_t^{EVR}) \tau_1 \\ & - \sum_{j \in G} \sum_{k \in G, j < k} Pr_{jk,t,\tau_1} g(ES_{jk,t} - P_t^{EVR}) \tau_1, \forall t \in T \end{aligned} \quad (19)$$

where the $EENS_t^I$, represented as (18), can be obtained by summarizing the expected energy deficit because of single unit outage and double unit outage within PEV reaction time τ_1 respectively. Considering the $EENS$ is a polynomial function of time τ , $EENS_t^{II}$ cannot be acquired directly. To obtain $EENS_t^{II}$, the first and second terms of (19) denote $EENS$ within system contingency time τ_2 based on the assumption that PEVs react immediately after contingency, while the third and fourth terms of (19) denote $EENS$ within time τ_1 with the assumption of PEVs' immediate participation. The capacity of the PEVs' contribution to operating reserve P_t^{EVR} is the sum of the PEVs' interruptible charging demand P_t^{V2G} and V2G capacity P_t^{V2G} , represented as,

$$P_t^{EVR} = P_t^{Int} + P_t^{V2G}, t \in T \quad (20)$$

The formulation of the three parameters P_t^{EVR} , P_t^{Int} and P_t^{V2G} will be introduced in the next section. Similar to the formulation of $EENS_t^{II}$, $EESEV_t^{Int}$ and $EESEV_t^{V2G}$ could be expressed as,

$$EESEV_t^{Int} = \sum_{j \in G} Pr_{j,t,\tau_2} g[\min(ES_{j,t}, P_t^{Int})] \tau_2$$

$$\begin{aligned}
 & + \sum_{j \in G} \sum_{k \in G, j < k} Pr_{jk,t,\tau_2} g[\min(ES_{jk,t}, P_t^{\text{int}})] \tau_2 \\
 & - \sum_{j \in G} Pr_{j,t,\tau_1} g[\min(ES_{j,t}, P_t^{\text{int}})] \tau_1 \\
 & - \sum_{j \in G} \sum_{k \in G, j < k} Pr_{jk,t,\tau_1} g[\min(ES_{jk,t}, P_t^{\text{int}})] \tau_1, \forall t \in T
 \end{aligned} \tag{21}$$

$$\begin{aligned}
 EESEV_t^{\text{V2G}} & = \sum_{j \in G} Pr_{j,t,\tau_2} g[\min(ES_{j,t} - P_t^{\text{int}}, P_t^{\text{V2G}})] \tau_2 \\
 & + \sum_{j \in G} \sum_{k \in G, j < k} Pr_{jk,t,\tau_2} g[\min(ES_{jk,t} - P_t^{\text{int}}, P_t^{\text{V2G}})] \tau_2 \\
 & - \sum_{j \in G} Pr_{j,t,\tau_1} g[\min(ES_{j,t} - P_t^{\text{int}}, P_t^{\text{V2G}})] \tau_1 \\
 & - \sum_{j \in G} \sum_{k \in G, j < k} Pr_{jk,t,\tau_1} g[\min(ES_{jk,t} - P_t^{\text{int}}, P_t^{\text{V2G}})] \tau_1, \forall t \in T
 \end{aligned} \tag{22}$$

where $EESEV_t^{\text{int}}$ and $EESEV_t^{\text{V2G}}$ are derived through that the supplied energy during the system contingency time τ_2 neglecting PEVs' reaction time, as the first and second terms in (21) and (22), subtracts the extra amount of supplied energy during PEV reaction time τ_1 , as the third and fourth terms in (21) and (22). As the cost of interrupting the PEV charging demand is quite smaller than the cost of providing V2G service, charging interruption would be preferentially conducted in practice. From the practical point of view, the possible scenarios can be listed as below:

- 1) If the spinning reserve can cover the capacity loss of system contingency, no energy deficit emerges and no PEVs react;
- 2) If the energy deficit is smaller than the total PEV interruptible capacity P_t^{int} , only part of charging energy is interrupted;
- 3) If the energy deficit is larger than the interruptible capacity P_t^{int} and smaller than total PEV capacity P_t^{EVR} , total charging energy is interrupted and part of V2G service is conducted;
- 4) If the energy deficit is larger than the total PEV capacity P_t^{EVR} , total charging capacity and total V2G capacity are scheduled to support power system. Only in this case, energy not supplied emerges.

C. Optimization Methodology

The formulated SRR optimization model is non-convex but unimodal because the system cost does not change continuously when an additional unit is turned on. The iterated grid search algorithm with three-grid points is applied here to solve the problem [29], with the details shown as Algorithm 1. In the algorithm, the interval $[Lb \ Ub]$ is first set large enough containing the optimal value of SRR in the first initialization step; then three points of SRR are acquired equably among the given interval in Step 5. Based on the searched SRR, generation cost is firstly optimized in Step 6; then EENS and EESEV are calculated in Step 7; the total system cost is obtained by summarizing the various costs at last in Step 8. Comparing the results, a narrower interval $[Lb \ Ub]$ is reset, as shown from Steps 10-16. This process is also visually illustrated in Fig. 2, where I_1 is selected as new optimization interval if $f_{SRR}(r_{t,m=1}^{\text{req}})$ is

the smallest, I_2 is selected as new optimization interval if $f_{SRR}(r_{t,m=2}^{\text{req}})$ is the smallest, and I_3 is selected as new optimization interval if $f_{SRR}(r_{t,m=3}^{\text{req}})$ is the smallest. The optimal SRR is finally obtained until Lb is close enough to Ub and used as inputs of reserve-constrained unit commitment.

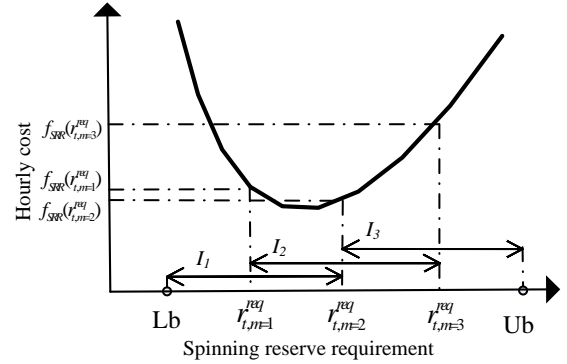


Fig. 2. Illustration of the iterated grid search algorithm

Algorithm 1 Grid search-based spinning reserve optimization methodology

- 1: **Initialization:** Set $t=1, k=1$. Set $I_k=[Lb \ Ub]$ large enough to contain the optimal value of SRR
 - 2: **for** $t=1$ to 24 **do**
 - 3: **while** $Ub-Lb>\epsilon$
 - 4: **for** $m=1$ to 3 **do**
 - 5: Let $r_{t,m}^{\text{req}}=Lb+m/4*(Ub-Lb)$
 - 6: Optimize $f_{\text{OPER}}(r_{t,m}^{\text{req}})$, as shown in (2), with constraints (5)-(10) to obtain $u_{i,t}^*, P_{i,t}$ and $r_{i,t}$
 - 7: Calculate $EENS_t, EESEV_t^{\text{int}}$ and $EESEV_t^{\text{V2G}}$ with (11)-(22)
 - 8: Calculate $f_{\text{EENS}}(r_{t,m}^{\text{req}})$ and $f_{\text{EESEV}}(r_{t,m}^{\text{req}})$ using (3)-(4) and then calculate $f_{\text{SRR}}(r_{t,m}^{\text{req}})$ using (1)
 - 9: **end for**
 - 10: **If** $f_{\text{SRR}}(r_{t,m=1}^{\text{req}}) < f_{\text{SRR}}(r_{t,m=2}^{\text{req}})$ & $f_{\text{SRR}}(r_{t,m=1}^{\text{req}}) < f_{\text{SRR}}(r_{t,m=3}^{\text{req}})$ **Then**
 - 11: Let $[Lb \ Ub]=[Lb \ f_{\text{SRR}}(r_{t,m=1}^{\text{req}})]$
 - 12: **Else if** $f_{\text{SRR}}(r_{t,m=2}^{\text{req}}) < f_{\text{SRR}}(r_{t,m=1}^{\text{req}})$ & $f_{\text{SRR}}(r_{t,m=2}^{\text{req}}) < f_{\text{SRR}}(r_{t,m=3}^{\text{req}})$ **Then**
 - 13: Let $[Lb \ Ub]=[f_{\text{SRR}}(r_{t,m=1}^{\text{req}}) \ f_{\text{SRR}}(r_{t,m=3}^{\text{req}})]$
 - 14: **Else if** $f_{\text{SRR}}(r_{t,m=3}^{\text{req}}) < f_{\text{SRR}}(r_{t,m=1}^{\text{req}})$ & $f_{\text{SRR}}(r_{t,m=3}^{\text{req}}) < f_{\text{SRR}}(r_{t,m=2}^{\text{req}})$ **Then**
 - 15: Let $[Lb \ Ub]=[f_{\text{SRR}}(r_{t,m=2}^{\text{req}}) \ Ub]$
 - 16: **End if**
 - 17: **End while**
 - 18: Set $r_t^{\text{req}}=1/2*(Ub-Lb)$
 - 19: **End for**
 - 20: Reserve-constrained unit commitment
-

III. MODELING OPERATING RESERVE PROVIDED BY PEVS

In this section, the operating reserve provided by PEVs is mathematically modeled. PEV travel behavior is firstly simulated. Then two different charging scheduling schemes are executed on basis of two typical charging strategies, i.e., immediate charging and smart charging strategy. The capacities of PEV interruptible charging demand and V2G service are calculated respectively. The costs of providing these two services including the compensation to PEV owners and battery degradation are formulated at last. It is worth mentioning that modeling capacity and cost of PEVs' service aims to estimate day-ahead PEVs' capacity to provide operating reserve, so that the day-ahead SRR can be optimized accordingly. The actual post-contingency dispatch of PEVs is dependent on the real-time PEV information obtained by the aggregator, which

is out of the scope of this paper.

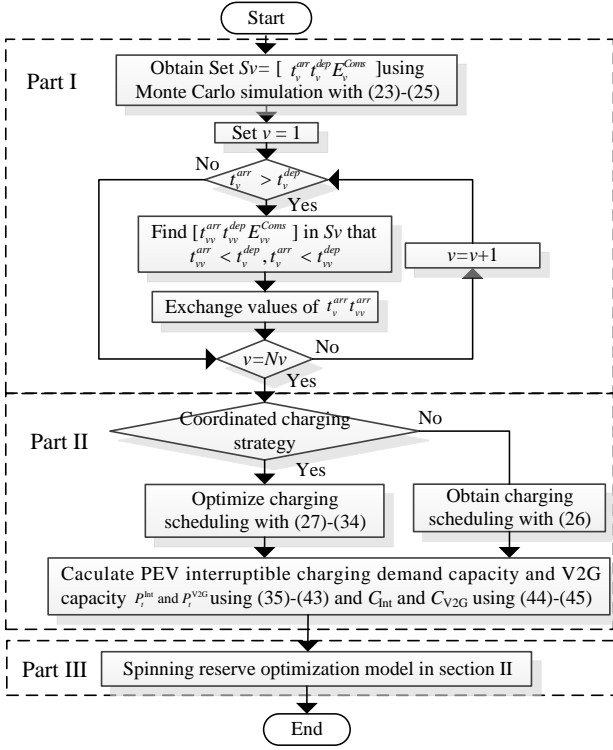


Fig. 3. Flowchart of modeling operating reserve provided by PEVs

A. PEV Travel Behavior Simulation

The PEV travel data is derived from the national household travel behavior survey, conducted by the U.S. Department of Transportation Federal Highway Administration [30]. A statistical probability method is conducted to analyze the results of travel behaviors [31, 32]. Segmented normal distribution functions are adopted to match the time when the EV first plugs out of the grid and the time when the electric vehicle last plugs into the grid. The probability density functions $f_s(t)$ and $f_e(t)$ are respectively represented in (23) with $\mu_s = 8.92$ and $\sigma_s = 3.24$, (24) with $\mu_e = 17.47$ and $\sigma_e = 3.41$.

$$f_s(t) = \begin{cases} \frac{1}{\sqrt{2\pi}\sigma_s} \exp\left[-\frac{(t-\mu_s)^2}{2\sigma_s^2}\right], & t \in [0, \mu_s + 12] \\ \frac{1}{\sqrt{2\pi}\sigma_s} \exp\left[-\frac{(t-24-\mu_s)^2}{2\sigma_s^2}\right], & t \in [\mu_s + 12, 24] \end{cases} \quad (23)$$

$$f_e(t) = \begin{cases} \frac{1}{\sqrt{2\pi}\sigma_e} \exp\left[-\frac{(t+24-\mu_e)^2}{2\sigma_e^2}\right], & t \in [0, \mu_e - 12] \\ \frac{1}{\sqrt{2\pi}\sigma_e} \exp\left[-\frac{(t-\mu_e)^2}{2\sigma_e^2}\right], & t \in [\mu_e - 12, 24] \end{cases} \quad (24)$$

The daily travel mileage is modeled using a logarithmic normal distribution function as below with $\mu_m = 2.98$ and $\sigma_m = 1.14$

$$f_m(x) = \frac{1}{\sqrt{2\pi}\sigma_m x} \exp\left[-\frac{(\ln x - \mu_m)^2}{2\sigma_m^2}\right] \quad (25)$$

The Monte Carlo simulation method is used to capture the travel behaviors of the vehicles according to the above

probability density functions $f_s(t)$, $f_e(t)$ and $f_m(t)$. The energy consumption before the vehicles are integrated into the grid is estimated according to the travel mileage and per mile energy consumption. The Monte carlo simulation is justified to make sure arriving time t_v^{arr} is smaller than the departure time t_v^{dep} , as shown in Part I in Fig. 3.

B. Charging Strategy

Different PEV charging strategies would have different effects on the ability of PEVs in providing the operating reserve at each time interval. Both typical immediate charging and smart charging strategies are considered in the study.

1) *Immediate Charging*: In the immediate charging mode, PEVs are assumed to be charged immediately after they are plugged into the grid when the last trips end in a certain day. The charging duration depends on the travel mileage during the day. Assuming that PEVs can respond to the contingency in several minutes, the intra-hour index τ is used to formulate a more precise model and set the interval as 10 minutes in the study. The PEV charging load can be given as,

$$P_{v,t,\tau}^{ch} = \begin{cases} P_{ch,max}, & \text{if } u_{v,t,\tau}^{EV} = 1 \text{ and } t + \tau \leq \frac{E_v^{Coms}}{\eta_{ch} P_{ch,max}} + t_v^{arr} \\ 0, & \text{if } u_{v,t,\tau}^{EV} = 0 \text{ or } t + \tau > \frac{E_v^{Coms}}{\eta_{ch} P_{ch,max}} + t_v^{arr} \end{cases} \quad \forall v \in V, \forall t \in T, \forall \tau \in T_\Delta \quad (26)$$

where $u_{v,t,\tau}^{EV}$ denotes the state whether PEV is connected to the grid; $P_{ch,max}$ represents maximum charging power; E_v^{Coms} denotes the daily energy consumption. Once PEV arrives, it is charged at the maximum rate $P_{ch,max}$ until the energy is full.

2) *Smart Charging*: In the smart charging mode, the travel information of each PEV, such as the travel time and the daily travel energy consumption, would be collected; then the time and the amount of PEVs' charging demand are orderly determined by the system operators or the PEV aggregators to benefit the operation of power systems. Here, a smart charging demand optimization model is proposed to optimize the PEVs' charging demand at each period through minimizing the daily system load fluctuation. Due to the large quantity of PEVs, a clustering method is used in this model to reduce the computation burden. The PEVs with similar pattern of travel time and the daily travel mileage could be classified into the same group, which can be dispatched as a whole. Electric vehicle smart charging strategy has been attracting lots of attentions in the research field of smart grid. To conduct smart charging strategy, lots of studies choose the objection of charging cost minimization in electricity market [20] or generation cost minimization [24]. In this paper, the objective is set as demand smoothing [33], which can be formulated as,

$$\min f_{co} = \sum_{t \in T} (P_t^{total} - P_{aver})^2 \quad (27)$$

where

$$P_t^{total} = P_t^D + \frac{1}{1000} \sum_{c \in V_c} \sum_{\tau \in T_\Delta} P_{c,t,\tau}^{ch,clus} \quad (28)$$

$$P_{\text{aver}} = \frac{1}{24} \sum_{t \in T} P_t^{\text{total}} \quad (29)$$

subject to:

$$S_{c,t+1}^{\text{clus}} = S_{c,t}^{\text{clus}} + \sum_{\tau \in T_{\Delta}} \frac{\eta_{ch} P_{c,t,\tau}^{\text{ch,clus}} \Delta \tau}{n_c S_{EV,\text{max}}}, \forall c \in V_c, \forall t \in [t_c^{\text{arr}}, t_c^{\text{dep}}] \quad (30)$$

$$S_{\text{clus,min}} \leq S_{c,t}^{\text{clus}} \leq S_{\text{clus,max}}, \forall c \in V_c, \forall t \in [t_c^{\text{arr}}, t_c^{\text{dep}}] \quad (31)$$

$$S_{c,t_c^{\text{dep}}}^{\text{clus}} \geq S_c^{\text{clus,exp}} \quad \forall c \in V_c \quad (32)$$

$$0 \leq P_{c,t,\tau}^{\text{ch,clus}} \leq \frac{1}{6} n_c P_{\text{ch,max}}, \forall c \in V_c, \forall \tau \in T_{\Delta}, \forall t \in [t_c^{\text{arr}}, t_c^{\text{dep}}] \quad (33)$$

$$P_{c,t,\tau}^{\text{ch,clus}} = 0, \forall c \in V_c, \forall \tau \in T_{\Delta}, \forall t \notin [t_c^{\text{arr}}, t_c^{\text{dep}}] \quad (34)$$

The objective defined in (27) is devoted to smoothing the daily system demand. The mathematical definitions of P_t^{total} and P_{mean} are expressed as (28) and (29) respectively. The equality constraint of charging energy of each cluster is shown as (30). The upper and lower limits of equivalent battery capacity of PEV clusters are defined by (31). The basic travel demand requirement should be satisfied as the inequality (32). The constraints of charging power limitation and non-schedulable state are listed as (33) and (34), respectively.

C. Capacity Estimation

Once the charging demand at each period is determined under either immediate charging strategy or smart charging strategy, the time-varying capacity of interruptible charging demand and V2G service can be obtained according to the specific values of the PEVs' parameters, including the charging demand, the arriving and departing time, energy remained in the PEV battery, etc. The details of this process can be referred to Part II in Fig.3.

The capacity of interruptible charging demand depends not only on the charging demand itself, but also on whether the interrupted load can be recharged before PEV's departure. In other word, the charging energy during system contingency can be interrupted only if there is still enough time to recharge this amount of energy between the recovery of system contingency and PEV's departure, which can be represented as,

$$P_t^{\text{Int}} = \zeta_t \frac{\sum_{v \in V} \min(E_{v,t'}^{\text{Ch}}, E_{v,t'}^{\text{Sup}})}{1000 \sum_{t' \in T} \sum_{\tau \in T_{\Delta}} (u_{t',t,\tau}^{\text{CII}} - u_{t',t,\tau}^{\text{EV,del}}) \Delta \tau}, \forall t' \in T \quad (35)$$

where

$$E_{v,t'}^{\text{Ch}} = \sum_{t \in T} \sum_{\tau \in T_{\Delta}} (u_{t',t,\tau}^{\text{CII}} - u_{t',t,\tau}^{\text{EV,del}}) P_{v,t,\tau}^{\text{ch}}, \forall v \in V, \forall t' \in T \quad (36)$$

$$E_{v,t'}^{\text{Sup}} = \sum_{t \in T} \sum_{\tau \in T_{\Delta}} u_{t',t,\tau}^{\text{CIII}} (u_{v,t,\tau}^{\text{EV}} P_{\text{ch,max}} - P_{v,t,\tau}^{\text{ch}}) \Delta \tau, \forall v \in V, \forall t' \in T \quad (37)$$

where $E_{v,t'}^{\text{Ch}}$ is the amount of total charging energy between when PEVs respond to contingency and when system recovers, $E_{v,t'}^{\text{Sup}}$ denotes the maximum amount of supplementary recharging energy between the time when power system recovers from contingency and the time when PEV departs, the time index t' is to indicate the time when the contingency happens. In this paper, system contingency is assumed to happen only at the beginning of each hour for simplicity. The definitions of the binary parameters $u_{t',t,\tau}^{\text{CI}}$, $u_{t',t,\tau}^{\text{CII}}$, $u_{t',t,\tau}^{\text{CIII}}$ and $u_{t',t,\tau}^{\text{EV,del}}$ are listed as,

$$\begin{cases} u_{t',t,\tau}^{\text{CI}} = 1, u_{t',t,\tau}^{\text{CII}} = 0, u_{t',t,\tau}^{\text{CIII}} = 0, & \text{if } t' < t + \tau \\ u_{t',t,\tau}^{\text{CI}} = 0, u_{t',t,\tau}^{\text{CII}} = 1, u_{t',t,\tau}^{\text{CIII}} = 0, & \text{if } t' \leq t + \tau < t' + \tau_2 \\ u_{t',t,\tau}^{\text{CI}} = 0, u_{t',t,\tau}^{\text{CII}} = 0, u_{t',t,\tau}^{\text{CIII}} = 1, & \text{if } t' + \tau_2 \leq t + \tau \end{cases} \quad (38)$$

$$\begin{cases} u_{t',t,\tau}^{\text{EV,del}} = 1, & \text{if } t' \leq t + \tau < t' + \tau_1 \\ u_{t',t,\tau}^{\text{EV,del}} = 0, & \text{if } t + \tau_1 \leq t' \text{ or } t' + \tau_1 \leq t + \tau \end{cases} \quad (39)$$

$$\begin{cases} u_{v,t,\tau}^{\text{EV}} = 1, & \text{if } t + \tau \in [t_c^{\text{arr}}, t_c^{\text{dep}}] \\ u_{v,t,\tau}^{\text{EV}} = 0, & \text{if } t + \tau \notin [t_c^{\text{arr}}, t_c^{\text{dep}}] \end{cases} \quad (40)$$

where $u_{t',t,\tau}^{\text{CI}}$, $u_{t',t,\tau}^{\text{CII}}$ and $u_{t',t,\tau}^{\text{CIII}}$ are the binary parameters with 1 denoting before, during and after contingency, respectively, $u_{t',t,\tau}^{\text{EV,del}}$ is the binary parameter with 1 denoting that the PEVs are reacting to contingency, $u_{v,t,\tau}^{\text{EV}}$ is the binary parameter with 1 indicating that PEV is connected to the grid. The number 1000 is used to make the transition from kW to MW.

The formulation of the V2G capacity is similar to (35). However, the discharging limitation and the energy remained in the battery of PEVs when V2G happens should be involved in the formulation of the V2G capacity as well, represented as,

$$P_t^{\text{V2G}} = \xi_t \frac{\sum_{v \in V} \min(E_{v,t'}^{\text{Rem}}, E_{v,t'}^{\text{V2G,lim}}, E_{v,t'}^{\text{Sup}})}{1000 \sum_{t' \in T} \sum_{\tau \in T_{\Delta}} (u_{t',t,\tau}^{\text{CII}} - u_{t',t,\tau}^{\text{EV,del}}) \Delta \tau}, \forall t' \in T \quad (41)$$

where

$$\begin{aligned} E_{v,t'}^{\text{Rem}} &= S_{EV,\text{max}} - E_v^{\text{Coms}} \\ &+ \sum_{t \in T} \sum_{\tau \in T_{\Delta}} (u_{t',t,\tau}^{\text{CI}} + u_{t',t,\tau}^{\text{EV,del}}) P_{v,t,\tau}^{\text{ch}}, \forall v \in V, \forall t' \in T \end{aligned} \quad (42)$$

$$E_{v,t'}^{\text{V2G,lim}} = \sum_{t \in T} \sum_{\tau \in T_{\Delta}} u_{v,t,\tau}^{\text{EV}} (u_{t',t,\tau}^{\text{CII}} - u_{t',t,\tau}^{\text{EV,del}}) P_{V2G,\text{max}} \Delta \tau, \forall v \in V, \forall t' \in T \quad (43)$$

where $E_{v,t'}^{\text{Rem}}$ defined in (41) denotes the total energy remained in the battery of PEVs before conducting V2G service, which can be derived by summing the energy remained in the battery and the charged energy when PEVs are connected to the grid before PEVs respond to the contingency to provide V2G service, $E_{v,t'}^{\text{V2G,lim}}$ defined in (42) represents the V2G energy limitation due to the limit of PEVs' V2G recharging power during PEVs' reaction period.

D. Cost of PEVs' Service

The PEV owners should be rewarded for the delay of charging caused by both the interruption and V2G. Besides, discharging a battery for providing V2G service will speed up its degradation procedure. Then the costs of interrupted charging demand C_{Int} and V2G service C_{V2G} can be respectively expressed as,

$$C_{\text{Int}} = C_{\text{Comp}} \quad (44)$$

$$C_{V2G} = C_{\text{Comp}} + \frac{1000 C_{\text{BI}}}{L_c S_{EV,\text{max}} d_{\text{DoD}}} \quad (45)$$

where C_{Comp} is the per MWh cost of compensation to PEV owners, and the second term of (44) is the per MWh investment cost of the battery degradation [33, 34], C_{BI} is battery investment cost of V2G service, L_c is the battery cycle life at a certain depth of discharge (DoD); $S_{EV,\text{max}}$ is the battery capacity;

d_{DoD} is the DoD used in determining L_C . Thus, $L_C S_{EV,max} d_{DoD}$ represents the overall energy that a battery can provide throughout its lifetime and the number 1000 is used to make the transition from \$/kWh to \$/MWh.

IV. CASE STUDY

The IEEE reliability test system (RTS -96) [35] is utilized to demonstrate the basic characteristics of the proposed PEV-integrated SRR model. The test system consists of 26 units and the hydro generating units are not taken into consideration in any of the case studies in this paper. The unit cost data is obtained from [36]. The load of the system varies from 59% to 100% of 2700 MW peak load, without consideration of the PEV charging demand. Other parameter settings are given in Table I. The values of the parameters τ_1 and τ_2 are set based on the interruptible import requirement and contingency reserve restoration requirement in Reliability Standards for the Bulk Electric Systems of North America [27]. The details of the battery degradation cost can be referred to [33]. The modeling of electric vehicle uncertainty parameter can be referred to [37].

TABLE I
PARAMETER SETTINGS

Parameters	Values	Parameters	Values
τ_1	1/6 h	V	10000
τ_2	1 h	$VOLL$	7500 \$/MWh
L_b	300 MW	C_{Comp}	125 \$/MWh
U_b	500 MW	$C_{BI}/S_{EV,max}$	100 \$/kWh
$P_{ch,max}$	4.5 kW	d_{DoD}	0.8
$P_{V2G,max}$	9 kW	L_C	1000
ω	1%	ε	1MW

For the future practical application, two kinds of uncertainties should be taken into consideration: whether V2G service and smart charging strategy can be fulfilled. Thus six scenarios are tested in the study, as shown in Table II. Total power system demand remains the same among Scenarios 1, 3 and 5 where Scenario 5 acts as benchmark for the other two scenarios. Similarly, the total demands of Scenarios 2, 4 and 6 are the same, and Scenario 6 is utilized as the benchmark.

TABLE II
SCENARIOS OF CASE STUDY

Scenario	1	2	3	4	5	6
V2G service	Enabled	Enabled	Not enabled	Not enabled	Not enabled	Not enabled
Charging interruption	Enabled	Enabled	Enabled	Enabled	Not enabled	Not enabled
Charging strategy	Immediate charging	Smart charging	Immediate charging	Smart charging	Immediate charging	Smart charging

A. Determination of Interruptible and V2G Capacity

The interruptible and V2G capacity with both immediate and smart charging strategies available for contingency can be demonstrated in Fig. 4. Generally, the V2G capacity is much larger than the interruption capacity as most of the PEVs connected on the grid have the ability to feed energy back to power system, while only small proportion of PEVs which are in charging conditions has the ability to interrupt charging energy. The V2G capacity demonstrates great difference during

the day and night as much more vehicles park at night. The interruption capacity varies a lot with different charging strategies. The energy charging is scheduled mostly at night under the smart charging strategy, and scheduled separately during the day under the immediate charging strategy.

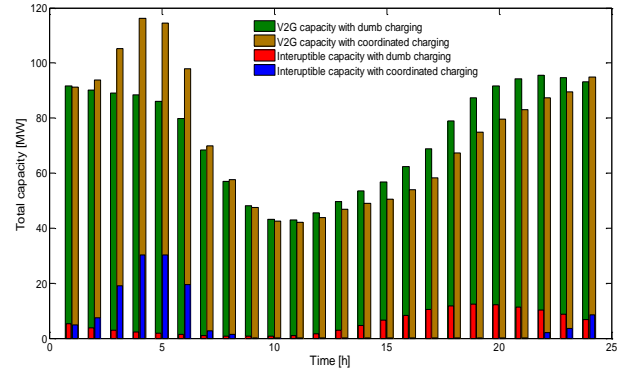


Fig. 4. Interruptible and V2G capacities with immediate and smart charging strategies.

B. Optimization Spinning Reserve Requirement

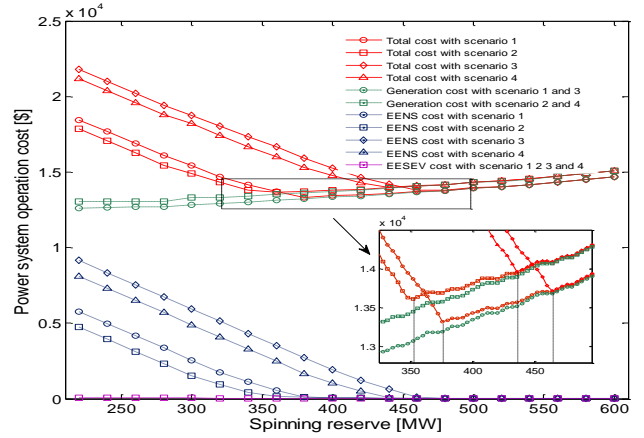


Fig. 5. Optimization of SRR with regard to the total cost, generation cost, EENS cost and EESEV cost when $t=4h$

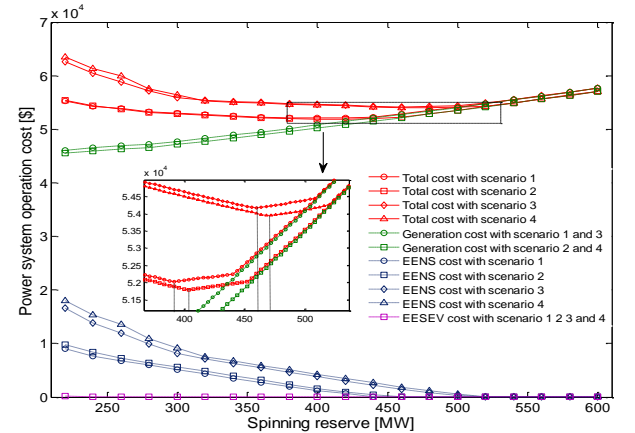


Fig. 6. Optimization of SRR with regard to the total cost, generation cost, EENS cost and EESEV cost when $t=18h$

In order to demonstrate how the SRR is obtained with the proposed model, various hourly costs, i.e., total system cost, generation cost, EENS cost and EESEV cost with different SRRs are depicted in Figs. 5 and 6. Only two typical time intervals $t=4h$ and $t=18h$ are selected respectively indicating

the lowest and highest the system demand during the whole day. The optimal SRR is acquired by reaching the minimization of the total cost, as shown in Figs. 5 and 6. The SRR is optimized through tradeoff among costs of generations, EENS and EESEV. It can be found that larger SRR results in larger generation costs and smaller SRR leads to larger EENS costs. It is proved that the function of total cost is unimodal and the grid search-based SRR optimization methodology can be valid to resolve the proposed cost-oriented optimization model. Generally, the system with larger demand would have larger SRR and larger system cost, through comparing the results depicted in Figs. 6 and Fig. 5. It can be also found that the SRR is considerably cut down when V2G service is enabled, and the SRR is smaller in the night and larger during the day under smart charging strategy comparing with immediate charging strategy.

C. Economic Efficiency Analysis

TABLE III
VARIOUS DAILY COSTS OF DIFFERENT SCENARIOS

Scenario	Total costs (\$)	Generation costs (\$)	EENS costs (\$)	EESEV costs (\$)
1	8.2027×10^5	7.9674×10^5	2.2501×10^4	1.0300×10^3
2	8.1988×10^5	7.9651×10^5	2.2303×10^4	1.0594×10^3
3	8.5088×10^5	8.2818×10^5	2.2665×10^4	32.4850
4	8.5041×10^5	8.2774×10^5	2.2643×10^4	28.4796
5	8.5408×10^5	8.3051×10^5	2.3571×10^4	0
6	8.5071×10^5	8.2786×10^5	2.2851×10^4	0

Daily system operation costs can be obtained once the reserve-constrained unit commitment is determined. Various costs of the studied six scenarios are listed in Table III. Comparing Scenarios 1 and 2 with Scenarios 5 and 6 respectively, the large reduction of the total costs solidly indicate the economic effectiveness of PEVs' aid in system operating reserve allocation. Particularly, the generation costs are considerably reduced from 8.3051×10^5 \$ to 7.9674×10^5 \$ under immediate charging strategy and from 8.2786×10^5 \$ to 7.9651×10^5 \$ under the smart charging strategy due to PEVs' contribution, and EENS costs also slightly decrease from 2.3571×10^4 \$ to 2.2501×10^4 \$ in the immediate charging strategy and from 2.2851×10^4 \$ to 2.2303×10^4 \$ in the smart charging strategy. On the other hand, the additional compensation costs and the battery costs that system operator should pay for EENS are relatively small, with 1.0300×10^3 \$ and 1.0594×10^3 \$ in the immediate and smart charging strategies respectively. It is because the frequency of activating PEVs to provide energy is quite low. Thus PEVs are very economically suitable to partly replace generators to provide contingency reserve. As the interruptible capacity is relatively smaller than the V2G capacity, the PEVs' system-supporting effectiveness without V2G is considerably reduced by comparing various costs of Scenarios 3 and 4 with Scenarios 5 and 6 respectively. The results also demonstrate larger benefit brought by the utilization of smart charging strategy. However, the difference value between total costs of Scenarios 1 and 2 is diminished compared with that between Scenarios 5 and 6. It demonstrates that the economic advantage of smart charging strategy is weakened if PEVs are required to provide operating

reserve. It is due to that PEVs in immediate charging strategy can provide more operating reserves separately during most of the time intervals, as shown in Fig. 4 and thus helps to reduce the operating costs. Thus the necessity to shift the charging demand as smart charging is largely weakened.

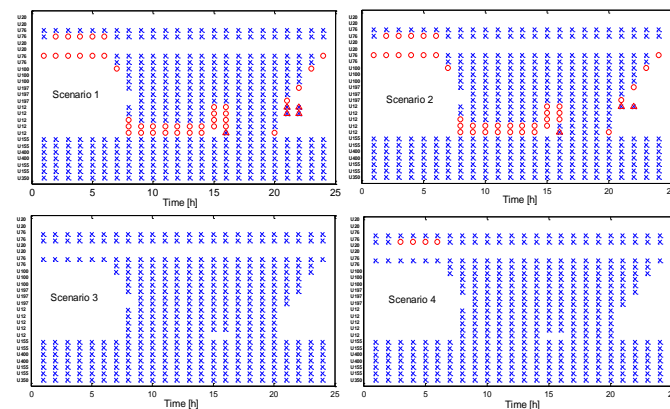


Fig. 7. Unit commitment under various scenarios

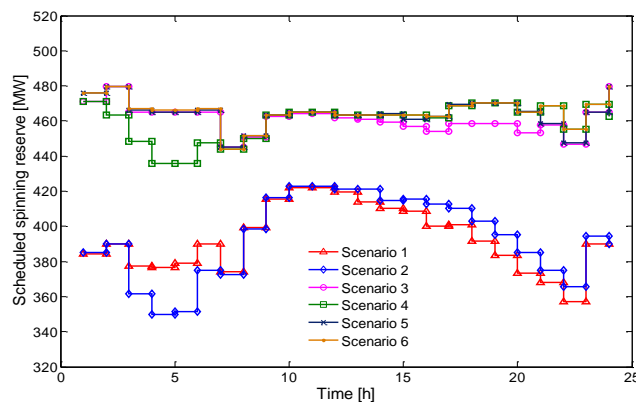


Fig. 8. Scheduled spinning reserve under various scenarios

D. Scheduled Spinning Reserve and Unit Commitment

Unit commitment under various scenarios is demonstrated in Fig. 7, with “x” denoting committed-on unit, “o” denoting turned-off unit opposite the benchmark and “Δ” denoting turned-on unit opposite the benchmark. Divided by different charging strategies, Scenario 5 acts as the benchmark of Scenarios 1 and 3 while Scenario 6 acts as the benchmark of Scenarios 2 and 4. The index per unit represents the generation capacity, for instance, U400 demonstrates the unit with installed capacity of 400 MW. Once the unit commitment is determined, the scheduled hourly spinning reserve under various scenarios can be also obtained, as shown in Fig. 8.

When PEVs are supposed to provide operating reserve, especially V2G service is enabled in Scenarios 1 and 2, some units with relatively small capacity are turned off compared to the corresponding benchmarks. For example, U76 is turned off in the night and U12 is turned off during the day. Nevertheless, several units, e.g., U12 at $t=16$ h, 21 h and 22 h, are turned on to partly compensate the vacancy left by the turned-off units with larger capacity, e.g., U197. The amount of scheduled spinning reserve is thus considerably reduced, shown as Scenarios 1 and 2 in Fig. 8. When system contingency happens, PEVs can

interrupt the charging demand and feed energy back to support the power system. Thus system operators do not need to schedule as much spinning reserve as before and some units can be turned off.

When only PEV interruption is enabled, the support of PEVs to power system is relatively small. In this condition, the unit commitment results are almost the same with benchmark and the amount of scheduled spinning reserve is just slightly smaller than the benchmark as shown in Scenarios 3 and 4 in Figs. 7 and 8, respectively. Under the immediate charging strategy in Scenario 3, the unit commitment is exactly the same with benchmark. However, the scheduled spinning reserve is smaller than the benchmark especially during the day. In this case, units with larger capacity, which are supposed to provide spinning reserve, are allowed to increase the outputs as the requirement of spinning reserve is reduced. Under the smart charging strategy, the interruptible PEV capacity is very large as most of PEVs are charged together at night. Thus some units, e.g., U78 at $t = 3$ h, 4 h, 5 h and 6 h, are turned off and the scheduled spinning reserve at night is reduced, shown as Scenario 4 in Figs. 7 and 8 respectively.

E. Improvement of Power System Reliability

The effects of PEVs on the power system reliability by interrupting charging demand and feeding energy back to power system when contingency happens are discussed here. Expected energy not supplied is regarded as one of the most important reliability assessment indices. The daily EENS values with different reactions of PEVs and different charging strategies are listed in Table IV. It is demonstrated that the daily EENS is reduced in Scenarios 1-4 comparing with the benchmarks Scenarios 5 and 6, which proves that the reliability of power system is improved due to the assistance from PEVs' post-contingency support. Comparing with the obtained results of other scenarios, Scenarios 1 and 2 have smaller EENS, indicating that V2G service can help to improve system reliability even more. It can be also seen that the smart charging strategy has advantages on enhancing the reliability by comparing Scenarios 1, 3 and 5 with Scenarios 2, 4, and 6 respectively.

TABLE IV
EENS OF DIFFERENT SCENARIOS

Scenario	1	2	3	4	5	6
EENS(MWh/day)	1.5001	1.4869	1.5110	1.5095	1.5714	1.5234

V. DISCUSSIONS OF FUTURE IMPLEMENTATIONS

In the previous sections, the effects of PEVs on the spinning reserve allocation in various scenarios are analyzed, given the specific rewards to the PEV users and the specific PEV penetration level. However, for the practical implementation in the future, these two factors will greatly affect the performance and efficiency of PEVs' participation in operating reserve allocation. Sensitivity analysis of PEV penetration level and compensation cost is conducted in this section.

A. Sensitivity Analysis of PEV Penetration Level

In order to address the uncertainty of PEV population in the

future, various case studies considering different PEV penetration levels are fulfilled. The penetration level of PEV charging load can be defined as,

$$PL_{PEV} = \frac{N_{PEV} P_{ch,max}}{P_{aver}} \times 100\% \quad (46)$$

The daily average scheduled spinning reserve is defined as the average value of hourly spinning reserve in one day, to efficiently assess the degree of daily spinning reserve. The average scheduled spinning reserve in different PEV penetration levels is depicted in Fig. 9. To make the figure clearer, Scenarios 5 and 6 are not drawn here as the average scheduled spinning reserves in these scenarios are not affected by PEV penetration level, with 464MW and 465MW respectively. The average scheduled spinning reserve decreases with the increase of PEV penetration level, according to the numerical results of Scenarios 1-4 from Fig. 9. The V2G service highlights this characteristic, as shown in Scenarios 1 and 2. Although the low penetration level demonstrates that PEV charging energy is only a small proportion of the total load of the power system, it has considerable effects on power system spinning reserve allocation. It is because the PEV interruptible and V2G capacity cannot be neglected compared with potential energy loss due to generation outage.

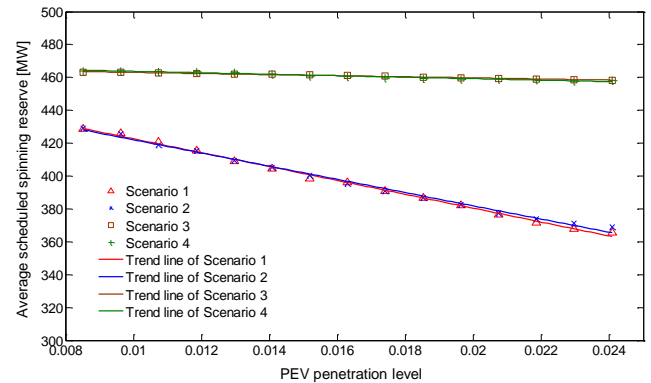


Fig. 9. Effects of PEV penetration level on scheduled spinning reserve

B. Sensitivity Analysis of Compensation Cost

The design of the compensation to the PEV owners would affect the motivation of providing operating reserve in the future. The sensitivity analysis of compensation cost is to find out the potential ability and monetary space for system operators to reward the PEV owners for their contributions. The index of compensation rate is defined as the ratio of the compensation cost to the scheduled generation marginal cost, given as,

$$CR_{PEV} = \frac{C_{Comp}}{\frac{1}{24} \sum_{i \in T} \frac{\partial f_{SRR}}{\partial P_{i,t}}} \times 100\% , \quad (47)$$

where unit i is the marginal generator.

Here the scheduled generation marginal cost is used to estimate the electricity price. The index of compensation cost is to roughly measure the degree of compensation from the view of users. The system total costs under various compensation rates with Scenario 1-4 are demonstrated in Fig. 10. The total costs of Scenarios 5 and 6, fixed as 8.5408×10^5 \$ and

8.5071×10^5 \$, are not affected by the compensation rate, which are not depicted in Fig. 10. The total cost generally increases with the compensation cost in the studies. However, the increasing speed is reduced with the increase of compensation rate especially for Scenarios 1 and 2. When the compensation rate reaches 350, the system total costs of Scenarios 1 and 3 get close to the cost of Scenario 5, 8.5408×10^5 \$, and the costs of Scenarios 2 and 4 are close to the cost of Scenario 6, 8.5071×10^5 \$. At these points, the compensation to PEV owners gets close to the value of VOLL, and PEV can no longer contribute to reduce the SRR and total operation cost. It can be demonstrated from the figure that the compensation rate is very high, as PEV owners will be rewarded with tens or hundreds times of the normal electricity price. It can be concluded that the system operators have the ability to pay PEV owners a large amount of rewards to motivate them to let their vehicles support the power system. Exact determination of the rewards will depend on further investigation in user willingness by e.g. questionnaire survey. The potential ability of power system operators to compensate PEV owners considerably enhances the possibility to implement the proposed model in the future.

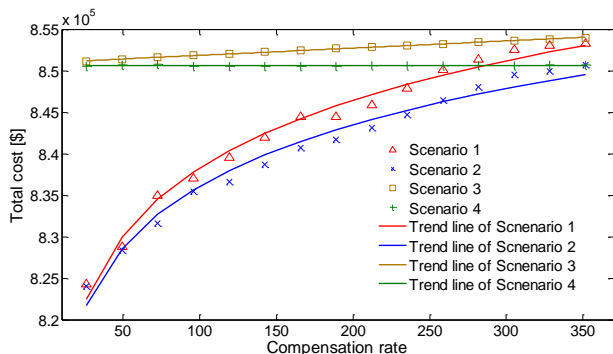


Fig. 10. Effects of compensation rate on total cost

VI. CONCLUSIONS

This paper proposes a novel cost-efficiency based SRR optimization model considering PEVs' assistance in providing operating reserve. EESEV is innovatively proposed to quantify the expected energy supplied by PEVs, with PEV reaction time taken into consideration. The optimal SRR is quantified based on the minimization of the total costs of generation operation, EENS and EESEV. Different charging strategies are considered in the determination of PEV charging demand as well as PEV interruptible and V2G capacities for reserve allocation purpose. Numerical case studies demonstrate the reduction of scheduled spinning reserve and the generation operation cost due to the support of PEVs. Unit commitment is rescheduled and some generators could be turned off as PEVs partly replace spinning reserve. The reliability of power system is also improved with PEVs' participation. The economic effectiveness of the proposed model will be significantly improved if V2G can be widely realized in the future. Furthermore, systematical sensitivity analysis implies that the amount of power system spinning reserve has a close relationship with PEV penetration level and there exists abundant space to improve the compensation rate to motivate PEV owners to provide power system operating reserve. In general, the proposed model can

have significant potential benefits for future practical applications.

REFERENCES

- [1] R. Allan, *Reliability evaluation of power systems*: Springer Science & Business Media, 2013.
- [2] C. Wan, Z. Xu, and P. Pinson, "Direct interval forecasting of wind power," *IEEE Transactions on Power Systems*, vol. 28, pp. 4877-4878, 2013.
- [3] A. J. Wood and B. F. Wollenberg, *Power generation, operation, and control*: John Wiley & Sons, 2012.
- [4] H. B. Gooi, D. P. Mendes, K. R. W. Bell, and D. S. Kirschen, "Optimal scheduling of spinning reserve," *IEEE Transactions on Power Systems*, vol. 14, pp. 1485-1492, 1999.
- [5] F. Bouffard and F. D. Galiana, "An electricity market with a probabilistic spinning reserve criterion," *IEEE Transactions on Power Systems*, vol. 19, pp. 300-307, 2004.
- [6] F. Bouffard, F. D. Galiana, and A. J. Conejo, "Market-clearing with stochastic security-part I: formulation," *IEEE Transactions on Power Systems*, vol. 20, pp. 1818-1826, 2005.
- [7] M. A. Ortega-Vazquez and D. S. Kirschen, "Optimizing the Spinning Reserve Requirements Using a Cost/Benefit Analysis," *IEEE Transactions on Power Systems*, vol. 22, pp. 24-33, 2007.
- [8] C. Wan, Z. Xu, P. Pinson, Z. Y. Dong, and K. P. Wong, "Probabilistic Forecasting of wind power generation using extreme learning machine," *IEEE Transactions on Power Systems*, vol. 29, pp. 1033-1044, 2014.
- [9] M. A. Ortega-Vazquez and D. S. Kirschen, "Estimating the Spinning Reserve Requirements in Systems With Significant Wind Power Generation Penetration," *IEEE Transactions on Power Systems*, vol. 24, pp. 114-124, 2009.
- [10] M. A. Matos and R. J. Bessa, "Setting the operating reserve using probabilistic wind power forecasts," *IEEE Transactions on Power Systems*, vol. 26, pp. 594-603, 2011.
- [11] S. Lou, S. Lu, Y. Wu, and D. S. Kirschen, "Optimizing spinning reserve requirement of power system with carbon capture plants," *IEEE Transactions on Power Systems*, vol. 30, pp. 1056-1063, 2015.
- [12] M. Jaefari-Nokandi and H. Monsef, "Scheduling of spinning reserve considering customer choice on reliability," *IEEE Transactions on Power Systems*, vol. 24, pp. 1780-1789, 2009.
- [13] J. Khorasani and H. R. Mashhadi, "Bidding analysis in joint energy and spinning reserve markets based on pay-as-bid pricing," *Generation, Transmission & Distribution, IET*, vol. 6, pp. 79-87, 2012.
- [14] J. Wang, X. Wang, and Y. Wu, "Operating reserve model in the power market," *IEEE Transactions on Power Systems*, vol. 20, pp. 223-229, 2005.
- [15] O. Nilsson, L. Soder, and D. Sjelvgren, "Integer modelling of spinning reserve requirements in short term scheduling of hydro systems," *IEEE Transactions on Power Systems*, vol. 13, pp. 959-964, 1998.
- [16] N. Chowdhury, "Energy method of spinning reserve assessment in interconnected generation systems," *IEEE Transactions on Power Systems*, vol. 8, pp. 865-872, 1993.
- [17] F. Aminifar, M. Fotuhi-Firuzabad, and M. Shahidehpour, "Unit Commitment With Probabilistic Spinning Reserve and Interruptible Load Considerations," *IEEE Transactions on Power Systems*, vol. 24, pp. 388-397, 2009.
- [18] D. Dallinger, D. Krampe, and M. Wietschel, "Vehicle-to-grid regulation reserves based on a dynamic simulation of mobility behavior," *IEEE Transactions on Smart Grid*, vol. 2, pp. 302-313, 2011.
- [19] E. Sortomme and M. A. El-Sharkawi, "Optimal scheduling of vehicle-to-grid energy and ancillary services," *IEEE Transactions on Smart Grid*, vol. 3, pp. 351-359, 2012.
- [20] R. J. Bessa and M. A. Matos, "Optimization Models for EV Aggregator Participation in a Manual Reserve Market," *IEEE Transactions on Power Systems*, vol. 28, pp. 3085-3095, 2013.
- [21] P. Sanchez-Martin, S. Lumbreras, and A. Alberdi-Alen, "Stochastic Programming Applied to EV Charging Points for Energy and Reserve Service Markets," *IEEE Transactions on Power Systems*, vol. 31, pp. 198-205, 2016.
- [22] M. R. Sarker, Y. Dvorkin, and M. A. Ortega-Vazquez, "Optimal Participation of an Electric Vehicle Aggregator in Day-Ahead Energy and Reserve Markets," *IEEE Transactions on Power Systems*, vol. PP, pp. 1-10, 2015.
- [23] C. Liu, J. Wang, A. Botterud, Y. Zhou, and A. Vyas, "Assessment of Impacts of PHEV Charging Patterns on Wind-Thermal Scheduling by

Stochastic Unit Commitment," *IEEE Transactions on Smart Grid*, vol. 3, pp. 675-683, 2012.

[24] M. Ghofrani, A. Arabali, M. Etezadi-Amoli, and M. S. Fadali, "Smart Scheduling and Cost-Benefit Analysis of Grid-Enabled Electric Vehicles for Wind Power Integration," *IEEE Transactions on Smart Grid*, vol. 5, pp. 2306-2313, 2014.

[25] Y. Ota, H. Taniguchi, T. Nakajima, K. M. Liyanage, J. Baba, and A. Yokoyama, "Autonomous Distributed V2G (Vehicle-to-Grid) Satisfying Scheduled Charging," *IEEE Transactions on Smart Grid*, vol. 3, pp. 559-564, 2012.

[26] H. Liu, Z. Hu, Y. Song, J. Wang, and X. Xie, "Vehicle-to-Grid Control for Supplementary Frequency Regulation Considering Charging Demands," *IEEE Transactions on Power Systems*, vol. 30, pp. 3110-3119, 2015.

[27] (Feb. 2016) North American Electric Reliability Corporation, Reliability Standards for the Bulk Electric Systems of North America [Online]. Available: <http://www.nerc.com/pa/Stand/Reliability%20Standards%20Complete%20Set/RSCCompleteSet.pdf>

[28] M Milligan and et al, "Operating Reserves and Wind Power Integration: An International Comparison," *National Renewable Energy Laboratory*, Oct. 2010.

[29] J. Kim, "Iterated grid search algorithm on unimodal criteria," *Ph.D.dissertation, Dept. Statist., Virginia Polytechnic Inst. and State Univ.,Blacksburg, VA., 1997.*

[30] A. Santos, N. McGuckin, H. Y. Nakamoto, D. Gay, and S. Liss, "Summary of Travel Trends: 2009 National Household Travel," *U.S. Department of Transportation Federal Highway Administration, Washington, DC, USA, Rep. FHWA-PL-11022, Jun. 2011.*

[31] W. Yao, J. Zhao, F. Wen, Y. Xue, and G. Ledwich, "A Hierarchical Decomposition Approach for Coordinated Dispatch of Plug-in Electric Vehicles," *IEEE Transactions on Power Systems*, vol. 28, pp. 2768-2778, 2013.

[32] J. Zhao, C. Wan, Z. Xu, and J. Wang, "Risk-based day-ahead scheduling of electric vehicle aggregator using information gap decision theory," *IEEE Transactions on Smart Grid*, vol. PP, pp. 1-10, 2015.

[33] G. Wang, J. Zhao, F. Wen, Y. Xue and Ledwich, G, "Dispatch Strategy of PHEVs to Mitigate Selected Patterns of Seasonally Varying Outputs From Renewable Generation," *IEEE Transactions on Smart Grid*, vol. 6, pp. 627-639, 2015.

[34] S.-L. Andersson, A. K. Elofsson, M. D. Galus, L. Goransson, S. Karlsson, F. Johnsson, *et al.*, "Plug-in hybrid electric vehicles as regulating power providers: Case studies of Sweden and Germany," *Energy Policy*, vol. 38, no. 6, pp. 2751-2762, Jun. 2010.

[35] P. Wong, P. Albrecht, R. Allan, R. Billinton, Q. Chen, C. Fong, *et al.*, "The IEEE Reliability Test System-1996. A report prepared by the Reliability Test System Task Force of the Application of Probability Methods Subcommittee," *IEEE Transactions on Power Systems*, vol. 14, pp. 1010-1020, 1999.

[36] C. Wang and S. M. Shahidehpour, "Effects of ramp-rate limits on unit commitment and economic dispatch," *IEEE Transactions on Power Systems*, vol. 8, pp. 1341-1350, 1993.

[37] N. Xu and C. Chung., "Uncertainties of EV Charging and Effects on Well-Being Analysis of Generating Systems," *IEEE Transactions on Power Systems*, vol. 30, pp. 2547-2557, 2015.

uncertainty analysis and operation, grid integration of renewable energies, demand side management, and machine learning.

Zhao Xu (M'06-SM'12) received his B.Eng., M.Eng, and Ph.D. degrees from Zhejiang University, China, in 1996, National University of Singapore, Singapore, in 2002, and The University of Queensland, Australia, in 2006, respectively.

He is now with The Hong Kong Polytechnic University. He was previously with Centre for Electric Power and Energy, Technical University of Denmark. His research interest includes demand side, grid integration of renewable energies and EVs, electricity market planning and management, and AI applications in power engineering. He is an Editor of *IEEE TRANSACTIONS ON SMART GRID*, *IEEE POWER ENGINEERING LETTERS*, and *Electric Power Components and Systems journal*.

Kit Po Wong (M'87-SM'90-F'02) obtained his M.Sc, Ph.D., and D.Eng. degrees from University of Manchester, Institute of Science and Technology, in 1972, 1974 and 2001 respectively.

Prof. Wong has been with the University of Western Australia, Perth, Australia, since 1974. He was Chair Professor and Head of Dept. of Electrical Engineering, The Hong Kong Polytechnic University. His current research interests include computation intelligence applications to power system analysis, planning and operations, stability and smart grids.

Prof. Wong received 3 Sir John Madsen Medals (1981, 1982, and 1988) from the Institution of Engineers Australia, the 1999 Outstanding Engineer Award from IEEE Power Chapter Western Australia, and the 2000 IEEE Third Millennium Award. He was General Chairman of IEEE/CSEE PowerCon2000 and IEE APSCOM 2003 and 2009. He is serving as the Editor-in-Chief of *IEEE POWER ENGINEERING LETTERS* and was Editor-in-Chief of *IEE PROC. GENERATION, TRANSMISSION & DISTRIBUTION*.

Jian Zhao (S'15) received the B.Eng. degree in Electrical Engineering from Zhejiang University, Hangzhou, China, in 2013. He is currently working toward the Ph.D. degree in the Department of Electrical Engineering, The Hong Kong Polytechnic University, Hong Kong.

His research interests include power system operation, demand response and electric vehicle.

Can Wan (M'15) received his B.Eng. and Ph.D. degrees from Zhejiang University, China, in 2008, and The Hong Kong Polytechnic University in 2015, respectively.

He is currently a Postdoctoral Research Fellow at Department of Electrical Engineering, Tsinghua University, Beijing, China. He was a Research Associate at Department of Electrical Engineering, The Hong Kong Polytechnic University, and a visiting PhD at the Center for Electric Power and Energy, Technical University of Denmark, and Department of Electrical Engineering, Tsinghua University. His research interests include power system